JOURNAL OF MATERIALS SCIENCE 28 (1993) 4037–4042

# HRTEM study of planar defects and polytypes in $MgSiO_3$

Y. G. WANG, Y. D. YU, H. Q. YE, W. K. HUANG*
*Laboratory of Atomic Imaging of Solids, Institute of Metal Research, Academia Sinica, Shenyang 110015, *and also Institute of Geochemistry, Academia Sinica, Guangzhou 510640, People's Republic of China*

The microstructure of a synthetic ceramic with the nominal composition of $MgSiO_3$ has been investigated by means of high-resolution transmission electron microscopy (HRTEM). Mistakes in stacking sequences, including an isolated fault and the coexistence of various stacking disorders resulting from the phase transition of high-temperature phase protoenstatite to room temperature phase clinoenstatite, have been determined. They consist of a sequential arrangement of the same kind of $SiO_3$ tetrahedral chains with identical and opposite skews, respectively. These stacking faults possibly formed during the early stage of nucleation of clinoenstatite on cooling. As a result, the new polytypes with repeat periods of 1.35 and 2.25 nm, respectively, perpendicular to the (1 0 0) plane were introduced by varying the stacking sequences in clinoenstatite and orthoenstatite matrix.

## 1. Introduction

Ceramics are being found in increasing use as electronic device components, function materials, composite materials and chemical engineering materials and thus are of potential interest in commercial manufacture. Magnesium and metasilicate ($MgSiO_3$), mineralogically called enstatite, is the major component of steatite ceramics which are used as electrical insulators. They have low power losses in the high-frequency range and good dielectric properties to elevated temperatures. Three phases in enstatite have been determined. They are a high-temperature phase protoenstatite (PEN) with unit cell parameters of $a = 0.92$ nm, $b = 0.889$ nm, $c = 0.520$ nm and space group $Pbcn$ stable above 1042 °C at ambient pressures, clinoenstatite (CLEN) with unit cell parameters of $a = 0.962$ nm, $b = 0.883$ nm, $c = 0.518$ nm, $\beta = 108.3°$ and space group $P2_1/c$ and orthoenstatite (OREN), constructed by CLEN in $b$-glide twinningrelated positions, with unit cell parameters of $a = 1.82$ nm, $b = 0.88$ nm, $c = 0.519$ nm and space group $Pbca$ stable at room temperature [1–4]. The polymorphism of enstatite has been extensively studied and summarized. The transformation mechanism between the three phases has been investigated. PEN produces OREN on slow cooling to room temperature. The slow PEN to OREN transformation mechanism is considered to be reconstructive. Fast quenching of PEN, however, introduces CLEN and the transformation mechanism has martensitic characteristics, being diffusionless, athermal, stress-inducible, and having an orientation relation between parent and product phases. Under hydrostatic stresses, the OREN to CLEN transformation is slow and sluggish, requiring the use of fluxes and long reaction times and it seems to be coincident with a non-martensitic mechanism [5–8]. In this paper the (1 0 0) stacking faults resulting from the disordering of $SiO_3$ tetrahedral chains, as well as the polytypes with repeat period of 1.35 nm perpendicular to the (1 0 0) plane, are presented.

## 2. Experimental procedure

The sample under investigation was prepared by solid to solid reaction. Chemically absolute MgO and $SiO_2$ powders were mixed according to the proportions $MgO:SiO_2 = 1:1$ and the powder mixture was pressed in a cylindrical mould at 150 MPa. The resultant compact pieces (about 15 mm diameter and about 10 mm thick) were finally heated in the platinum container in a platinum–rhodium-wound alumina muffle furnace. No special steps were taken to control the furnace atmosphere, but evidence from other preparations for which the furnace had been used showed that reducing conditions were unlikely to occur [9, 10]. Initially the mixture was fired at progressively higher temperature from 500 °C in 20 °C steps. The mixture was sintered at 1190 °C for 10 h. The sintered specimen was then rapidly quenched from 1190 °C to room temperature in air after withdrawal from the furnace and therefore it can be predicted that the PEN to CLEN transformation would be dominant and CLEN is the more abundant phase in this sample. X-ray examination showed the presence of CLEN and OREN. This ceramic was quite strong and brittle so that it was very easy to grind it into fine fragments in an agate mortar. The ultrasonic vibrator was used to disperse the fragments in absolute alcohol. Thin fragments of the ceramic were put on a carbon film

0022–2461  

supported on a copper grid. HRTEM was undertaken to examine the microstructure on an ultrafine scale and a JEM-200CX electron microscope equipped with an ultra-high-resolution pole piece (spherical aberration coefficients $C_s = 1.2$ mm) and top-entry goniometer stage was used at 200 kV. High-resolution electron micrographs were recorded at a direct magnification of $3.8 \times 10^5$–$8.5 \times 10^5$ times, using an objective aperture corresponding to a radius of 3.5 $nm^{-1}$ in the diffraction pattern. The exposure times were chosen as less than 4 s in order to avoid specimen draft due to mechanical and electrical instability. Various crystals oriented in $\langle 0\, v\, w \rangle$ directions were selected so that the images always include the (1 0 0) plane, which makes it easy to identify the (1 0 0) stacking faults as well as new polytypes belonging to such planar defects. All high-resolution images were taken under the symmetrically incident conditions according to the image simulation.

## 3. Results and discussion

### 3.1. (1 0 0) Stacking faults in CLEN

Figs 1a and 2a are [0 1 0] projected structures of CLEN and OREN, respectively. The most obvious structural feature of enstatite is the single chain of corner-sharing tetrahedra having $SiO_3$ stoichiometry. These chains are articulated to strips of edge-sharing polyhedra that are occupied by cations. In these enstatite structures, the octahedral strips and tetrahedral chains form layers parallel to (1 0 0). These layers can be stacked in various ways, leading to different enstatite polytypes when the stacking sequence is periodic. In CLEN there are two symmetrically distinct chains designated Si(A) and Si(B), respectively, whereas four chains denoted Si(A), Si(B), Si(A)′ and Si(B)′ are included in OREN, where primed and unprimed chains indicate opposite skews. These characters have been illustrated in projected structures. The simulated image calculations were performed using the multislice method with a program written by Ishizuka [11] in order to interpret experimental images unambiguously. The following parameters were used. Spherical aberration coefficient $C_s = 1.2$ mm, slice thickness 0.44 nm (half-length of $b$-axis), the focus spread due to chromatic aberration 7 nm, area limited by objective aperture 3.5 $nm^{-1}$, semi-angle of convergence of the incident beam 0.3 m rad, and the number of diffraction beams included in the dynamical diffraction calculation 121 and 213, respectively. The images were computed for a range of thickness up to 40 slices over a defocus range of $-40$ to $-90$ nm. A through-focus series of the high-resolution images were found in good agreement with the simulated ones calculated for varied defocus and Figs 1b and c and 2b and c are two pairs of them. The results of image simulation shows that each bright spot in the image taken at Scherzer defocus ($\Delta f = -65$ nm) corresponds to the channels surrounded by metal, oxygen and silicon atoms in structural models (Figs 1a and 2a). For comparison, the unit cells are outlined and the one to one correspondence of observed and simulated images shows that the image obtained under Scherzer condition could be interpreted and the presence of plane defects can be read directly. Fig. 3 is an electron diffraction pattern with the electron beam parallel to the [0 1 0] direction, in which the (1 0 0) twinning of CLEN and streaks along [1 0 0]* can be found. Fig. 4 is the corresponding high-resolution image showing intimate intergrowth of OREN and CLEN with the multiple unit cell twinning feature. The periods of these two phases correspond to even layers of $SiO_3$ tetrahedron chains.

In addition to these two basic structures, various (1 0 0) lamellae with different periods caused by the (1 0 0) stacking faults of $SiO_3$ tetrahedral chain have also been detected. Fig. 5 is a [0 1 0] high-resolution image, where a (1 0 0) isolated stacking fault can be identified. Based upon the fundamental structure of CLEN the possible stacking faults can be suggested as follows: Si(A)Si(B)Si(B)Si(A), Si(B)Si(A)Si(A)Si(B), Si(A)-Si(B)Si(B)′Si(A), Si(B)Si(A)Si(A)′Si(B)*, Si(B)Si(A)Si(B)′-Si(A)* and Si(A)Si(B)Si(A)′Si(B). These isolated stacking faults can be divided into three classes in terms of the sequences and skews of adjacent $SiO_3$ layers: first is the same kind of $SiO_3$ chains with the same skew stacked sequentially, e.g. the first two cases listed above, the second is the same two $SiO_3$ chains with

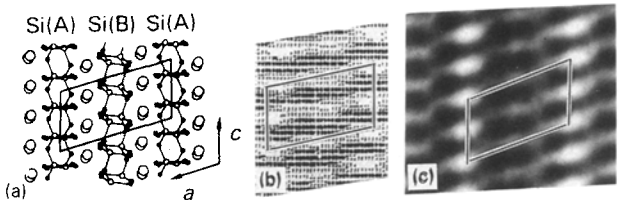


*Figure 1* (a) [0 1 0] projection of CLEN, where large and small circles and black dots represent magnesium, silicon and oxygen, respectively; (b) the simulated images calculated at a thickness of 8.8 nm and a defocus value of $-6.5$ nm based on the multislice method using 121 diffraction beams in computation, and (c) the experimental image.

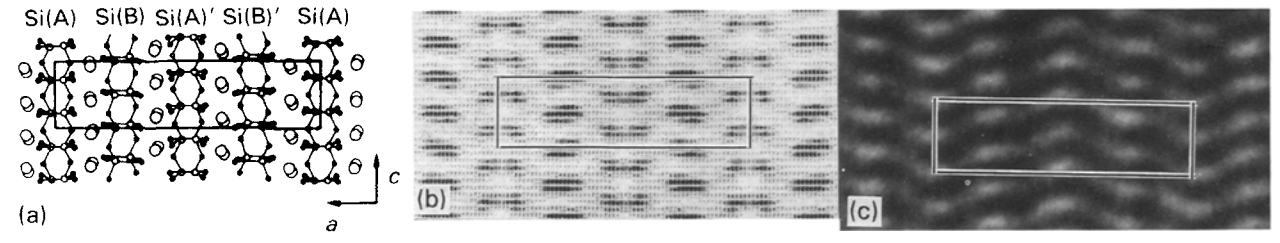


*Figure 2* (a) [0 1 0] projected structure of OREN, the different circles and dots have the same meaning as Fig.1a, (b) computer-generated image in the same conditions as Fig. 1b, using 213 diffraction beams in the calculation, and (c) the observed image.

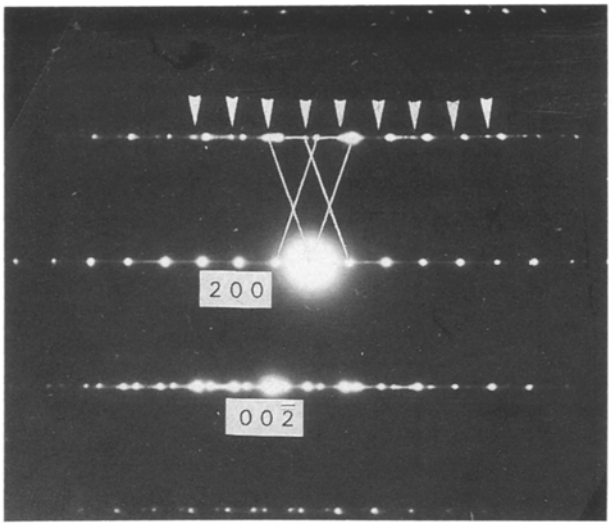


*Figure 3* An electron diffraction pattern with the electron beam parallel to the [0 1 0] axis showing the (1 0 0) twinning of CLEN and streaks along the [1 0 0]* direction; the arrows point to twin reflections.

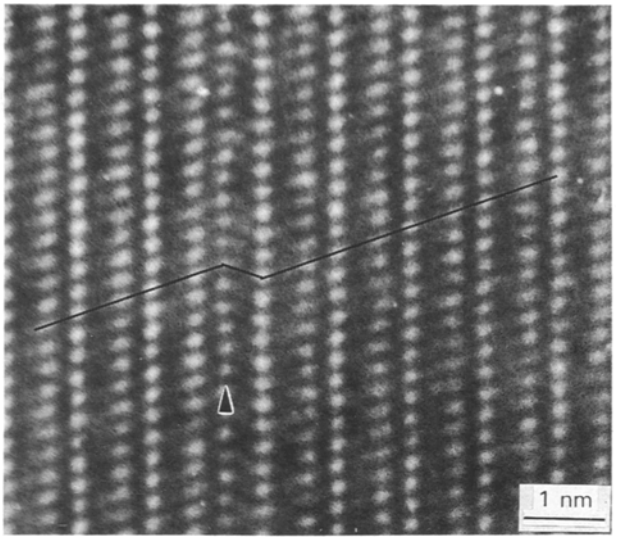


*Figure 5* [0 1 0] structural image illustrating the presence of an isolated (1 0 0) stacking fault in CLEN.

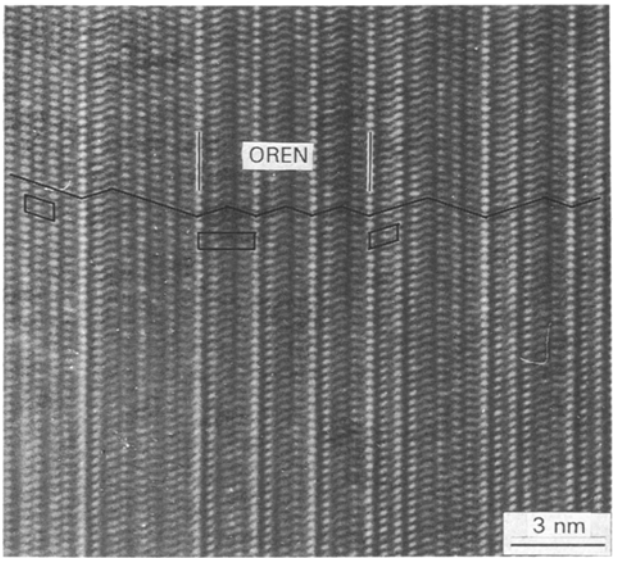


*Figure 4* [0 1 0] structural image exhibiting the intergrowth of CLEN with microtwin features and OREN.

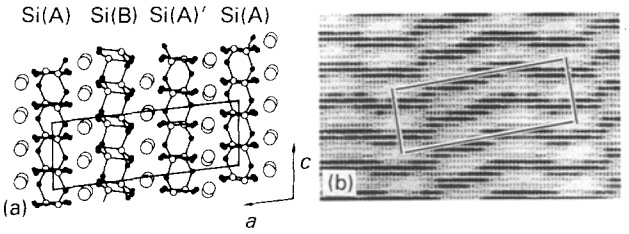


*Figure 6* (a) Schematic diagram of a (1 0 0) stacking fault caused by the same two $SiO_3$ layers with opposite skews in CLEN, and (b) the simulated image calculated for the same conditions as in Fig. 1b; 179 diffraction beams were included in the calculation.

opposite skews, e.g. third and fourth listed, and the third is an $SiO_3$ chain with opposite skew in regular stacking sequence of CLEN, e.g. the last two listed. The two faults indicated by asterisks have been predicted by Livi and Veblen [12]. The out-of-phase boundaries will be caused in the first and third cases, whereas the antiphase boundaries could be introduced in the second case. It should also be pointed out that only the possibly faulted stacking sequences of the $SiO_3$ layer are listed. The distortion at the faulted planes in real structures is not included in the following discussion. From the image simulation, the structural models of the (1 0 0) planar defect in Fig. 5 can be suggested and is shown in Fig. 6a. It corresponds to the continuous arrangement of the same two $SiO_3$ layers with opposite skews, and the corresponding simulated image (Fig. 6b) calculated at a thickness of 8.8 nm and a defocus value of $-67$ nm is also displayed. The calculated images match well with the experimental images and show that the structural models may be creditable to some extent. In this case, the same kind of chains with opposite skews are in (1 0 0) mirror reflection positions, respectively, with a twin plane at the cation plane so that the antiphase boundaries may be introduced by such arrangements of $SiO_3$ sheets. On the other hand, a different (1 0 0) planar defect has also been detected. Fig. 7 is also an [0 1 0] structural image exhibiting the (1 0 0) stacking fault, at which an isolated stacking fault can be seen and the configuration is different from Fig. 5. The possible model has been proposed and shown in Fig. 8a. In this case the two Si(B) types of $SiO_3$ chain come into being, and thus the out-of-phase boundary could be caused. Based upon this model, the simulated image (Fig. 8b) calculated under the same conditions as above was obtained and shows a good correspondence with the observed one. The genetic aspects of these stacking faults may result from the homogeneous nucleation of CLEN during the phase transition on cooling. In this process the homogeneous nucleation of CLEN with random skews could form in a PEN matrix. If two variants of CLEN with alternative arrangement of $SiO_3$ layers mix together, the (1 0 0) stacking faults consisting of a continuous arrangement of the same kind of $SiO_3$ chains with the same skew, can be formed. The isolated faults related to the skews of adjacent $SiO_3$ layers may also be produced because the disordering of skews of $SiO_3$ chains could be

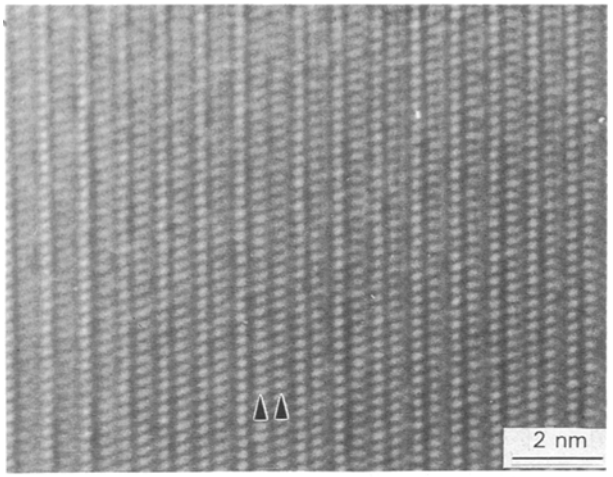


*Figure 7* [0 1 0] structural image showing an isolated stacking fault in CLEN.

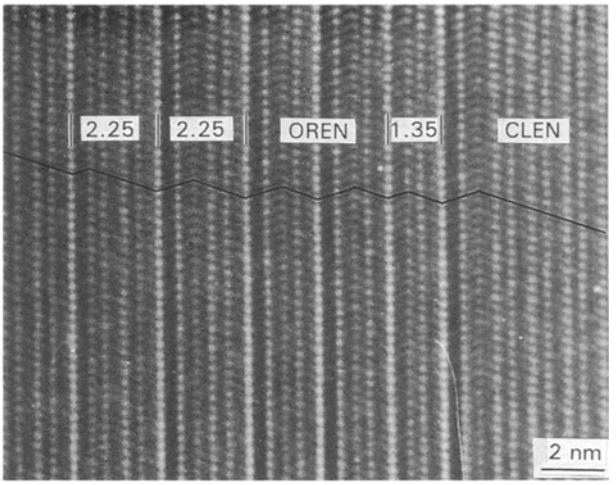


*Figure 9* [0 1 0] structural image depicting the coexistence of CLEN and OREN with stacking faults as indicated.

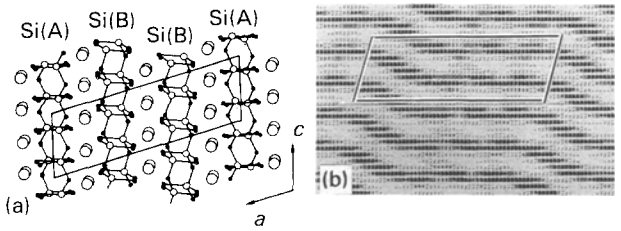


*Figure 8* (a) Schematic diagram of a mistake in the stacking sequence in the ideal structure of CLEN, involving the same two $SiO_3$ tetrahedral chains stacked continuously, and (b) the simulated image obtained for the same conditions as Fig. 6b.

predicted during the phase transition. The homogeneous nucleation of CLEN could be formed everywhere in the host on cooling so that the different interfaces between these CLEN lamellae may possibly be produced and various stacking faults would be introduced for the disordering of sequences and skews of $SiO_3$ sheets.

## 3.2. (1 0 0) Planar defect in OREN

OREN with a stacking disorder has also been found, although CLEN is the more abundant phase. Fig. 9 presents the [0 1 0] structural image of the coexistence of CLEN and OREN with (1 0 0) stacking faults. Three planar defects are indicated and the stacking faults on the left and right sides correspond to the case of opposite skews of adjacent $SiO_3$ layers as in Fig. 5, but the sequence of stacking faults on the right side agrees with Si(B)Si(B)′ type, whereas that on the left agrees with Si(A)Si(A)′. Based upon the results of image simulation, the stacking fault in the middle can be proposed as shown in Fig. 10a. It consists of two layers of the same two $SiO_3$ tetrahedral chains with the same skew, i.e. two Si(B)′ chains stacked sequentially in OREN. The simulated image (Fig. 10b) worked out for the same conditions as Fig. 2b shows good correspondence with the experimental image. In this case, an out-of-phase interface can be predicted between the adjacent layers on the two sides of the boundary as in Fig. 7. The transition mechanism from PEN to OREN is reconstructive, which involves changes in the stacking sequences of the polyhedral layers, and it is possible to introduce such a (1 0 0) faulted layer of the $SiO_3$ chain. On the other hand, this stacking fault may also be produced in process of PEN to CLEN transition and remained during further transition to OREN. The transition of PEN to CLEN was well advanced; therefore, it may be possible that this planar fault was produced at pre-phase transition.

## 3.3. Polytypism in enstatite

Polytypism is essentially one-dimensional polymorphism. The important differences between polytypes occur along one crystallographic axis. These differences are produced by varying the stacking sequences of structurally and chemically similar units. Dimensional relationships perpendicular to the stacking direction are almost constant. Because of the layered character of the enstatite structure parallel to (1 0 0), it is also possible that other ordered stacking sequences could occur, producing yet more enstatite polymorphs. Fig. 11 shows the [0 1 0] electron diffraction pattern demonstrating the presence of a new polytype in the CLEN matrix by the two extra spots appearing at 1/3 and 2/3 between transmission and the 2 0 0 spots of CLEN, and suggesting that the stacking period of this new polytype is 1.35 nm in real space, corresponding to the width of three $SiO_3$ layers. The lattice parameters calculated from this pattern are $a = 1.378$ nm, $b = 0.883$ nm, $c = 0.518$ nm, $\beta = 96.29°$, and it has nearly the same extinction conditions as CLEN, so that the space group $P2_1/c$ could be suggested. Such predictions are confirmed by the corresponding high-resolution image (Fig. 12), where alternative stacking orders consisting of mistakes in the regular stacking sequence of CLEN are found to be coincident with that in Fig. 5. Periodical repetition of such a stacking order introduces a new polytype with a repeat period of 1.35 nm. The periodic appearance of one unit cell sheet of CLEN and such a new

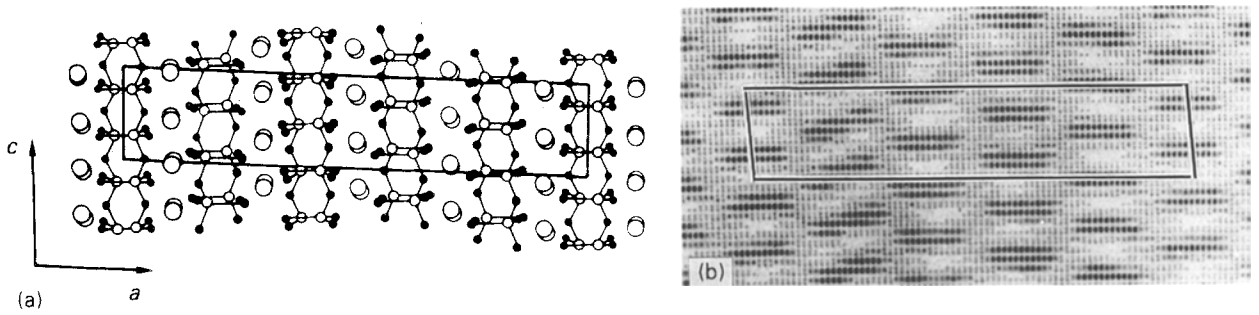


*Figure 10* A suggested structural model of (1 0 0) faulted stacking sequence of $SiO_3$ tetrahedral layers in OREN and (b) the simulated image computed for the same conditions as in Fig. 2b; 232 diffraction beams were included.

TABLE I The derived crystal data of new polytypes caused by stacking faults in enstatite

| Sequences of $SiO_3$ tetrahedral layer | Lattice parameters[a] |
|---|---|
| Si(A)Si(B)Si(B)Si(A) | $a = 1.443$ nm, $\beta = 108.3°$ |
| Si(B)Si(A)Si(A)′Si(B) | $a = 1.378$ nm, $\beta = 96.29°$ |
| Si(A)Si(B)Si(A)Si(B)′Si(B)′Si(A) | $a = 2.279$ nm, $\beta = 93.02°$ |

[a] $b$ and $c$ parameters are the same as the parent phases and are omitted in the table for briefness.

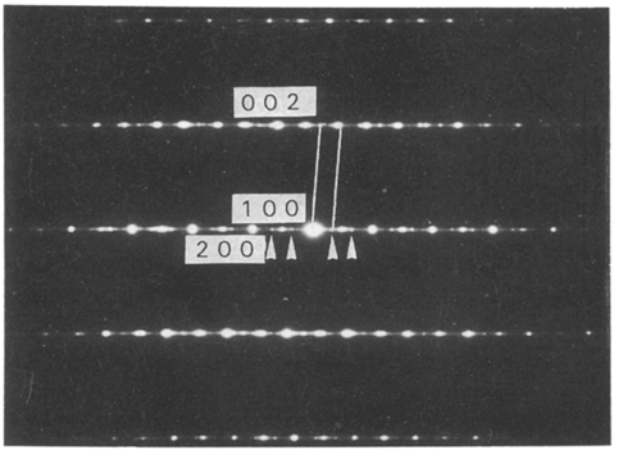


*Figure 11* An electron diffraction pattern with the electron beam projected along the [0 1 0] direction demonstrating a polytype with a repeat period of 1.35 nm by the appearance of two extra spots mid-way between the transmission and the 2 0 0 spots of CLEN.

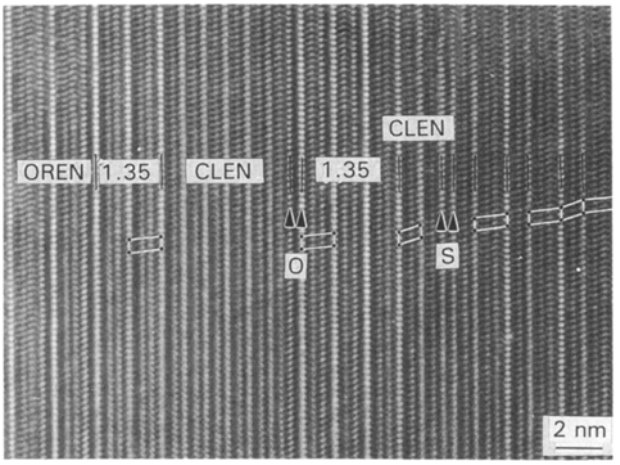


*Figure 12* [0 1 0] high-resolution image illustrating a new polytype with a stacking period of 1.35 nm; the possible unit cells are outlined for comparison. Two stacking faults are indicated by arrows at areas S and O, respectively.

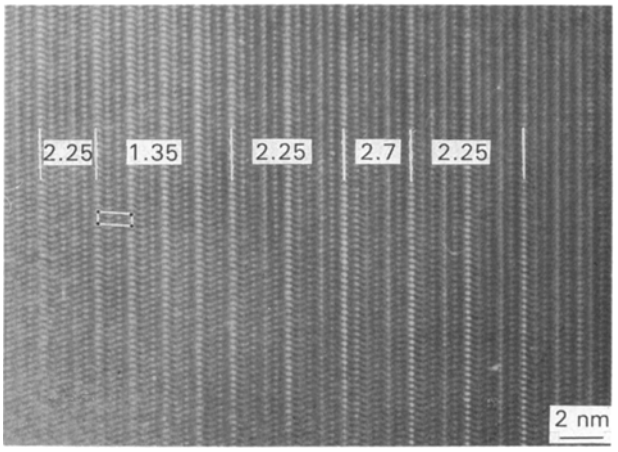


*Figure 13* [0 1 0] high-resolution image illustrating the coexistence of various polytypic lamellae with repeat periods of 1.35, 2.25 and 2.7 nm in turn.

polytype is also shown on the right-hand side of image. Therefore, a polytype with a period of 2.25 nm may also be predicted. The stacking faults possibly coincident with Si(A)Si(A)′ and Si(A)Si(A) types are also exhibited and marked by arrows at S and O areas, respectively, in the same figure. Fig. 13 is also a [0 1 0] high-resolution image showing the close intergrowth of polytype with periods of 1.35, 2.25 and 2.7 nm, respectively. These lamellae and others in Figs 7 and 9, may be described as single unit cells of new polytypes with a stacking period of 1.35, 2.25 and 2.7 nm, respectively, although such order stacking formation of lamellae in CLEN and OREN only contain a few or even one unit cell. The crystal data of these possibly new polytypes can be derived from the suggested structural models and summarized in Table I. The origin of polytypism within enstatite may have a close relationship to the phase transition of PEN to CLEN or OREN. On cooling, the nucleation of CLEN occurred everywhere within the PEN matrix and various stacking disorders as well as out-of-phase and anti-phase boundaries could be caused when these CLEN lamellae joined together. As a result, new polytypes were introduced for the periodical presence of such faulted stacking sequences or boundaries in local areas. The coexistence of these polytypes causes the

mistakes in the stacking sequence of $SiO_3$ layers and produces enstatite with a stacking disorder; the degree of disorder can range from isolated faults occurring in an otherwise ordered polytype as in Figs 5, 7, and 9, to a high density of stacking disorder as in Figs 12 and 13.

In superstructures, the polytypism may also be introduced by a lattice modulation wave that modifies the basic structure. The generally accepted picture of the lattice modulation wave can be divided into two types in terms of the structural aspect, i.e. spatially continuous or spatially discontinuous types. The former is a displacive-type modulation wave which has been reported for many materials [13, 14]. On the other hand, the latter is a non-displacive type and has been reported for many alloys and oxides and sulphides, which is usually accompanied by periodic or non-periodic arrays of crystal defects, such as out-of-phase boundaries [15–17]. In the present case, it is obvious that the superstructures or new polytypes agree with a spatially discontinuous type. These new phases may be formed by introducing the (1 0 0) stacking faults, i.e. the same two $SiO_3$ tetrahedral chains with the same and opposite skews, respectively, stacked sequentially at the initial stage of nucleation of CLEN.

## 4. Conclusion

It has been shown in HRTEM images that stacking disorder widely present in enstatite and more than two of the ideal structure-types may be found intergrown together in the same crystal, and thus an enstatite could be constructed with a completely random stacking sequence, resulting in complete lack of periodicity in the stacking direction. Such deviation from perfect periodicity and certain aspects of the phase transformation that commonly result in this structural disorder could be understood by an HRTEM method that supplies much vital information on characteristic features of the varying stacking sequences on a very fine scale. The disordering of $SiO_3$ layers may be introduced in the product phase in synthetic $MgSiO_3$ ceramic material because when enstatites cool from the temperatures at which they form, they undergo structural changes in order to remain in equilibrium. As a consequence, many enstatite crystals contain, within their structures, traces of the phase transition. Crystals that are not perfectly periodic may result. In this study, several sorts of polymorphic transformations occurred in enstatite; polytypic variations in enstatite structure and the way that the polytype was initiated have been revealed. The homogeneous nucleation of CLEN with an alternative arrangement of $SiO_3$ chains and random skews has been examined, so that the various out-of-phase and antiphase boundaries in the product phase could be produced between the adjacent $SiO_3$ sheets. Ordering of such interfaces in CLEN forms a lattice modulation wave that modifies the fundamental structure perpendicular to the (1 0 0) plane and, as a result, new polytypes with a repeat period of one and one-half times that of fundamental structures may be introduced. Such a faulted layer remaining in OREN may also cause a new polytype with a repeat period of 2.25 nm. Many of these features are both periodic and non-periodic and occur on a very small scale, so that HRTEM, which provides great spatial resolution of structural irregularities, has become a powerful and widely used technique for the study of enstatite microstructures. Using HRTEM, a rich variety of microstructures including the intergrowth of CLEN and OREN consisting of the perfectly periodic structure types and several types of deviations from perfect periodicity, for example isolated mistakes in the ideal stacking sequences, resulting in stacking faults, has been detected.

## References


1. J. R. SMYTH, *Z. Kristallogr.* **134** (1971) 262.
2. J. V. SMITH, *Acta Crystallogr* **12** (1959) 515.
3. N. MORIMOTO, *Z. Kristallogr.* **114** (1960) 120.
4. N. MORIMOTO and K. KOTO, *ibid.* **129** (1969) 65.
5. P. R. BUSECK, and S. IIJIMA, *Amer. Mineral.* **60** (1975) 771.
6. S. IIJIMA and P. R. BUSECK, *ibid.* **60** (1975) 758.
7. J. R. SMYTH, *ibid.* **59** (1974) 345.
8. P. R. BUSECK and D. R. VEBLEN, *Bull. Mineral.* **104** (1981) 249.
9. P. E. HALSTEAD and A. E. MOORE, *J. Appl. Chem.* **12** (1962) 413.
10. Y. G. WANG, H. Q. YE, K. H. KUO, X. J. FENG, G. L. LAO and S. Z. LONG, *J. Mater Sci.* **25** (1990) 5147.
11. K. ISHIZUKA, *Acta Crystallogr* **14** (1982) 80.
12. J. T. K. LIVI and D. R. VEBLEN, *Amer. Mineral* **74** (1989) 1070.
13. M. IIZUMI, J. D. AXE, G. SHIRANE and K. SHIMAOKA, *Phys. Rev.* **B15** (1977) 4392.
14. Van J. LANDUYT, Van G. TRNDLOO and S. AMELINCKX, *Phys. Status Solidi* **A36** (1976) 757.
15. S. IIJIMA and J. M. COWLEY, *J. Phys.* **C7** (1974) 135.
16. H. SATO and R. S. TOTH, *Phys. Rev.* **124** (1961) 1833.
17. H. NAKAZAWA, A. YAMAMOTO and M. MORIMOTO, in "Modulated Structures", edited by J. M. Cowley, AIP (American Institute of Physics) Conference Proceedings No. 53, New York (1979) p.358



*Received 7 February*
*and accepted 8 December 1992*